Enhancing COVID-19 Detection in X-Ray Images Through Deep Learning Models with Different Image Preprocessing Techniques

Ahmad Nuruddin bin Azhar[1], Nor Samsiah Sani[2] , Liu Luan Xiang Wei[3]
Center for Artificial Intelligence Technology-Faculty of Information Science and Technology,
Universiti Kebangsaan Malaysia, Selangor, 43600, Malaysia[1, 2, 3]

***Abstract*—The identification of COVID-19 using chest X-ray (CXR) images plays a critical role in managing the pandemic by providing a rapid, non-invasive, and accessible diagnostic tool. This study evaluates the impact of different image preprocessing techniques on the performance of deep learning models for COVID-19 classification based on COVID-19 Radiography Database, which includes 10,192 normal CXR images, 6012 lung opacity (non-COVID lung infection) images, and 1345 viral pneumonia images. Along with the images, corresponding lung masks are also included to aid in the segmentation and analysis of lung regions. Specifically, three convolutional neural network (CNN) models were developed, each using a distinct preprocessing method: Contrast Limited Adaptive Histogram Equalization (CLAHE), traditional histogram equalization, and no preprocessing. The results revealed that while the CLAHE-enhanced model achieved the highest training accuracy (93.26%) and demonstrated superior stability during training, it showed lower performance in the validation phase, with validation accuracy of 91.31%. In contrast, the model with no preprocessing, which exhibited slightly lower training accuracy (92.98%), outperformed the CLAHE model during validation, achieving the highest validation accuracy of 91.50% and the lowest validation loss. The histogram equalization model demonstrated performance similar to that of CLAHE but with slightly higher validation loss and accuracy compared to the unprocessed model. These findings suggest that while CLAHE excels in enhancing image details during training, it may lead to overfitting and reduced generalization ability. In contrast, the model without preprocessing showed the best generalization and stability, indicating that preprocessing techniques should be chosen carefully to balance feature enhancement with the need for generalization in real-world applications. This study underscores the importance of selecting appropriate image preprocessing techniques to enhance deep learning models' performance in medical image classification, particularly for COVID-19 detection. Histogram Equalization The results contribute to ongoing efforts to optimize diagnostic tools using AI and image processing.**

Keywords*—*X-ray; COVID-19; image enhancement; Contrast Limited Adaptive Histogram Equalization; Histogram Equalization

I. INTRODUCTION

The COVID-19 pandemic has caused dramatic global changes, both in healthcare and in our daily lives. One major challenge is the efficient identification of COVID-19 patients, where chest imaging has played a crucial role. While computed tomography (CT) scans provide high-resolution 3D images, their high cost and time requirements make them less practical than chest X-rays (CXR) for widespread use. Furthermore, COVID-19 has single-handedly become the driving force to so many unprecedented changes to the norms of today's modern society. On the flip side of things, we have observed welcomed acceleration in the adoption of digitalisation into our daily lives. This includes opening markets for online video meetings which in turn encouraging work from home policies and forcing countries into a standstill to fulfil lockdown requirements which leads to the reduction of carbon emissions by 8.8% (much larger than carbon emission reduction after World War II)[1][7]. Still, COVID-19 in its essence, is an unwelcomed pandemic that have brought tremendous amounts of varying losses (3.5 million deaths globally as of December 2019)and should be combated to the very best of humanity's capabilities [2][8] . Machine learning is one of the newest additions to our arsenal in fighting off COVID-19. We have seen efforts to direct the creation of effective policies, utilising the power of data to govern available resources through the means of analysis such as effectiveness of vaccines, rate of vaccination and rate of cases to identify COVID-19 hot spots. Chest imaging is one of the methods used to identify potential COVID-19 patients. Options include computed tomography (CT), X-ray and ultrasound scans. CT scans are images produced by a procedure of combining series of X-ray scans from multiple angles combined to create a 3D view. CT scans have the advantage of providing a better overview of a patient's conditions. However, it is considerably more expensive compared to X-ray procedures due to the much higher cost of the machine used as well as the time required to complete it. Deep learning models have shown promise in analyzing CXR scans to detect lung abnormalities linked to COVID-19, providing a faster, more accessible diagnostic tool. Previous studies have explored models with high accuracy, but few have investigated how different image preprocessing techniques can impact model performance. Attempts have been made in the past to provide assistance in identifying COVID19 patients with the use of transfer learning with MobileNet, obtaining an accuracy score of 96.33% as well as using the latest Generative Adversarial Network (GAN) on X-ray images obtaining 85% and 95% accuracy for dataset without and with data augmentation respectively [3], [4],[9],[10].

Abhishek Agnihotri and Narendra Kohli first proposed a novel 20-layer CNN model with an accuracy of 89.67 in order to analyze the performance of hybrid deep learning models versus novel deep learning models [6] and pre-trained models [21]. This model performs better than four pre-trained models

(Inception_ResnetV2, VGG16, VGG19 and InceptionV3) and achieves accuracy close to that of one pre-trained model (ResNet50). In order to narrow the gap in covid-19 severity prediction, Fares Bougourzi et al. proposed two methods based on 2D and 3D CNNS respectively. The proposed method is 36% more effective in predicting the severity of Covid-19 than the baseline method and represents a 14% improvement over the baseline method [22]. Dandil andYildirim proposed that the Mask R-CNN method was successful in the segmentation of COVID-19 infection, and COVID-19 infection on CT slices of open data sets was successfully segmented. In the experimental study, the scores of DSC, JSC, Precision and Recall were 81.93%, 74.19%, 90.27% and 79.47%, respectively [23]. Hammad and Khotanlou propose a simple CNN-based deep learning model, called Grad-CAM CNN (GCNN), to detect infection with COVID-19 disease through chest X-ray images and visualize heat maps with the help of Grad-CAM technology. In order to determine which area of chest X-ray images had COVID-19, a binary classification of normal chest X-ray images and positive chest X-ray images was performed, and the accuracy rate of detecting COVID-19 infection was 97.78%. Under the premise that the number of high-quality positive chest X-ray images was insufficient, they used a composite dataset to overcome this limitation [24].

Khadija developed a web-based online COVID-19 detection service, and the proposed FACNN framework enabled us to achieve precision, accuracy, sensitivity, F-measure, recall rate, and specificity to achieve high performance [25]. Arul Raj. A.M and Sugumar R demonstrated the feasibility of early identification of COVID-19 using cnn and pre-processed X-ray images, The COVID-19 detection method based on convolutional neural networks (cnn) and pre-processed chest X-ray images provides a promising solution for the accurate and efficient diagnosis of COVID-19 cases. The image quality and contrast are improved by image normalization, contrast stretching and segmentation, and the performance of CNN model is enhanced. Trained CNN models can generate accurate and efficient diagnostic reports, enabling healthcare professionals to quickly diagnose COVID-19 cases and take appropriate action [26].

Maddula et al. trained on a simplified large data set based on cnn, and the accuracy efficiency of the obtained model was 0.9835, precision was 0.915, sensitivity was 0.963, specificity was 0.972, and F1 score was 0.987. With ROC AUC of 0.925, this model is better than Random Forest with accuracy of 0.8997 and Naive Bayes with accuracy of 0.887, which proves that CNN's model can be combined with reinforcement learning for pattern recognition and deep learning model for processing large amounts of data. The above methods are helpful to improve the prediction accuracy [27]. Jagadeesh Marusani proposes a computer vision model to detect the presence of covid-19 infection and the location of the infection in the lungs. The proposed CNN model shows good performance on chest X-ray data sets and validation of different data sets. This model is smaller in size and requires six times fewer parameters to train. Compared to the most advanced EfficientNetB7 model, it is comparable and sometimes even shows better results [28]. Renuka Devi SM et al. used deep learning methods to train database images. When given a specific chest X-ray image as input, the system detects whether the X-ray is in the COVID-19 category or the normal category. The experimental results show that the accurate and accurate results obtained by CNN in COVID-19 detection are the best, with an accuracy rate of 96.8% [29]. Hassam Tahir et al. applied ResNet-101 to the local Covid-19 patient registration data set in order to facilitate infection of the virus in developing countries without vaccination facilities and to save time for rapid treatment of COVID-19 patients. Data from 8009 local chest radiographs were collected. Three neural networks were suggested for patients Faster R-CNN, Mask-CNN and ResNet-50. The faster R-CNN showed the best accuracy at 87 percent. The Mask RCNN was 83% accurate and the resNet-50 was 72% accurate [30]. Jing Zhang et al., because existing models do not apply to the three classifications of health controls, CP, and COVID-19. A novel diagnostic model for COVID-19 patients based on graph-enhanced three-dimensional convolutional neural networks (CNN) and cross-central domain feature adaptation is proposed. A 3D CNN with graph convolution module is designed to enhance the capability of global feature extraction. At the same time, a domain adaptive feature alignment method was used to optimize the feature distance between different centers to effectively realize multi-center COVID-19 diagnosis. Our experimental results achieved a fairly good COVID-19 diagnosis with 98.05% accuracy in the mixed dataset and 85.29% and 87.53% accuracy in cross-center tasks [31].

Several studies have explored the use of machine learning to detect COVID-19, achieving high accuracy with models trained on medical images. However, few have investigated how different image preprocessing techniques might impact the performance of these models. This study contributes to this gap by developing deep learning models based on various preprocessing techniques applied to CXR images. The preprocessing methods include Contrast Limited Adaptive Histogram Equalization (CLAHE), traditional Histogram Equalization, and a control model with no preprocessing.The contributions of this study are listed as follows:

1) Development of three CNN models: The study develops CNN models to classify COVID-19 using different image preprocessing techniques (CLAHE, Histogram Equalization, and no preprocessing).

2) Use of real CXR datasets: The dataset used consists of real X-ray images from the COVID-19 Radiography Database, obtained from open sources like Kaggle, and includes a large number of CXR images classified into COVID-19, normal, lung opacity, and viral pneumonia categories.

3) Identification of the most effective preprocessing method: The study identifies key preprocessing techniques that significantly influence model performance in detecting COVID-19, with Histogram Equalization emerging as the best method for model generalization.

In this paper, we aim to extend existing efforts by evaluating the impact of these preprocessing techniques on deep learning models for COVID-19 detection. Our approach follows a systematic comparison to determine which technique most effectively enhances model performance for detecting COVID-19 from chest X-rays.

II. Literature Review

A. X-ray Scans for COVID-19 Identification

Various methods have been proposed and applied in the global effort to mitigate the propagation of COVID-19. Given the limited knowledge base and database of the novel virus during the pandemic's inception, methods to identify potential patients mainly revolve around high recall with low costs (low material cost and lower expertise requirement) such as take-home test kits and clinical Antigen Rapid Test Kit (RTK). Another approach to identifying COVID-19 patients is by performing X-ray scans to identify COVID-19 related lung abnormalities by locating lung opacities (opaqueness of white areas within lung X-ray scans). The findings in Liqa A. Rousan's paper collected X-ray scans using portable Xray units based on anteroposterior projections [11]. A minority (31%) of the positive patients involved in the study was observed to possess or develop abnormalities on their chest X-ray (CXR) scans while 75% of the patients did not even though all of them are tested positive for COVID-19 using RT-PCR, the golden standard for COVID-19 testing. However, significant correlation was identified between the progression of abnormalities and symptoms experienced by patients with lung abnormalities, suggesting plausibility of judging patient's condition progress by judging changes of abnormalities in the X-ray scans. Common locations for the opacities are the peripheral and right lower zone of the lungs, with their respective distribution being 90% and 70%. Still, the paper suggested that X-ray scans still can be helpful in helping the process of diagnosing possible patients. Improvements could be made in future attempts to replicate the experiment conducted by having a much larger dataset compared to the one that was used in the paper with a total of 190 scans only. The baselines for judging progression of lung opacity should also include nonCOVID-19 patients to provide more comparisons for better identification of lung abnormalities unique to COVID-19.

A similar study has also been performed on pediatric patients, where a total of 44 patients tested positive based on PCR test were included as test subjects for CXR scans [12]. Results show that only a minority of the children tested (13.6%) has no observable findings in their scans. The most common lung abnormality observed was peribronchial cuffing (86.3%), a radiologic sign of excessive build-up of fluid and mucus small airway passages. This form of malformation is commonly found in the centre of CXR scans (81.8%) followed by 63.3% for peripheral occurrences. However, peribronchial cuffing should not be considered as definitive sign of COVID19 according to the authors as it is a shared observation with other viral pneumonias such as H1N1 influenza, adenoviruses, respiratory syncytial viruses, rhinoviruses and other coronaviruses [13]. Despite suggestions from the American College of Radiology (ACR) on not using CXR as the frontline test to diagnose COVID19, the paper stressed on the importance on performing CXR on pediatric patients who are at higher risks. This can greatly help in identifying target groups that require close medical monitoring, ultimately reducing fatality cases.

Both papers share the same limitation which is lack of data available which limits the possibility of performing a robust experiment to obtain definitive conclusions on the usability and practicality of CXR scans as a method to mitigate COVID-19.

B. Deep Learning as a Method to Classify X-Ray Scans for Covid-19

As surmised above, CXR should not be used as the primary tool to diagnose patients for COVID-19 due to the lack of decisive characteristics that can be used to single out COVID19 lung malformation compared to other pneumonia related diseases. However, findings from papers utilising deep learning for the purpose of classifying CXR scans displayed promising practical use prospect. With dataset added with augmented data, Abdul Waheed's GAN model boasted 95% accuracy [10]. Another paper also demonstrated excellent accuracy results in classifying X-Ray scans using various deep learning models such as DenseNet201(98.8%), InceptionV3(97.5%) and ResNet101(97.91%) [14]. These findings indicate that deep learning models can capture enough distinguishing patterns in lung abnormalities to train itself to become a high performing classifier. It should be addressed that since the classifier is a trained computer program, it can perform observations across large amount of data and is more capable at discerning and identifying unique identifiers of COVID-19 induced lung malformations. Still, this could not be fully used as an argument for the superiority of deep learning over human experts as there are no post model fitting activities performed that includes forms of validation or performance comparison between these models with human experts.

There are several image pre-processing methods that can be performed on the training dataset to enhance the defining features of COVID-19 induced lung abnormalities [15]. One commonly used image pre-processing method is to resize input images before feeding them into the model for training. This helps in speeding up the training process (by scaling down high-definition images) as well as standardizing input dimension. Image segmentation can also be performed to isolate the lungs from its background, theoretically removing irrelevant noises from being picked up as features by focusing on the Region of Interest (ROI). Another option is to perform image enhancements that enhance defining features of deformations. For this use case, histogram equalization can be used to distribute pixel intensity level. The referred paper suggested the use of Contrast Limited Adaptive Histogram Equalization (CLAHE) as it remedies the downside of using plain Adaptive Histogram Equalization which have the possibility to increase noise intensity in homogenous areas (areas with similar pixel values).

Increasing dataset is one of the popular ways to increase the performance of deep learning models. Considering the relatively young age of the COVID-19 pandemic, there is a scarcity of available datasets. Addition of augmented data can remedy this problem. It should be noted that augmentation is only performed on training datasets to avoid contaminating test datasets that are used for validation with artificial data. Options for augmentation include positional, colour and noise injection. These variations in data adds to the trained model's capability to learn from a more generalised, near to real life data that it will eventually try to classify during its application.

C. Image Pre-processing Methods to Enhance Input Features

Enhancing images as a part of data pre-processing is important in the application of CNN as the features learned are highly reliant on distinguishing features detected from input images. Improving the features of these images via removal of noise or blur and increasing contrast will help in improving spatial features, thus helping CNN models to learn better [10]. Still, the application of image enhancement must be performed in a way that will not affect information contained within the images. Altered features may lead to false learning, which in return will have a negative impact on the final model output. Various methods of image enhancements have been proposed to help improve classification models.

A paper on enhancing images used a fuzzy grayscale enhancement method to address low contrast due to inadequate lighting during capture [17]. The method used succeeded in improving image quality whilst also requiring relatively minimal processing time compared to other techniques. The proposed technique is performed by maximizing fuzzy measures within input images. Power-law transformation and saturation operator is then used to alter the membership function (a curve that defines how each point in the input space is mapped to membership value between 0 and 1) associated with the images.

A four stage image enhancing solution has also been proposed by M.Selvi and Aloysius George namely pre-processing, fuzzy based filtering, adaptive thresholding followed by morphological operation [18]. The stages are created to help pinpoint pixel areas and improve them using Fuzzy based filtering technique and adaptive thresholding. Resulting images are enhanced to have better peak signal-to-noise (PSNR) values compared to other filtering techniques at the time of the paper being written maps, etc., by exploiting similarity and semantic relationships. The nonlinear representation is further exploited in exploring web image search results.

III. Methodology

A. Data Preparation

The dataset used in this paper is obtained from Kaggle, titled COVID-19 Radiography Database [14], [16]. The dataset can be found using the following link: https://www.kaggle.com/datasets/tawsifurrahman/covid19radiography-database. The images are from four health condition classes namely COVID-19, normal (healthy), lung opacity (non-COVID lung infection) and viral pneumonia. Total number of images for each class are 3616, 10192, 6012 and 1345 respectively. Totalling the numbers gives us 21165. This dataset is built by researchers from Qatar University and the University of Dhaka, Bangladesh along with their collaborators from Pakistan and Malaysia. Sources include padchest dataset, a Germany medical school, Github, SIRM, Kaggle and Tweeter. The images are X-Ray scan results from patients subjected to the scan for the purpose of detecting COVID-19. The CNN model will be used to perform feature extraction on these images and use the characteristics identified in input feature maps for the purpose of classification. Based on the abnormalities present in the chest X-ray scans, the CNN model will then be able to perform the necessary predictions. The augmented training data generation for the CNN model was performed using the Keras ImageDataGenerator class with several parameters passed for the purpose of data augmentation. Data augmentation is a method that increases the amount of data artificially by creating new sets of data derived from geometric transformations applied on the original dataset. Alterations include forms of rotation, translation, flipping and noise addition. Forms of alteration such as adjusting brightness or applying ZCA whitening is not considered. Instead, minor width and height shift is applied to account for possible positions at which the lung and corresponding abnormalities are located within the X-ray scans. Horizontal flip is also enabled, while vertical flip is not. This means, the model will not take into consideration an upside-down X-Ray scans as well as forego any significance put into the positions of pneumonia induced lung malformations. In simpler words, any abnormalities formed either at the right or the left side of the CXR scans are considered to have the same significance in classifying the respective CXR scans.

As highlighted above, the distribution of data for each class is not balanced, with normal X-ray scans consisting almost half of the entire dataset. This was not addressed as initially considered in favour of maintaining the amount of learnable data over possible bias. Dropping these images with the purpose of balancing the dataset may lead to a reduction of performance as the pool of data that the model can learn from reduces. Geometric transformations are not applied to the data due to the sensitive dependence on pixel locations as well as the minute variations that accounts for the difference in the X-ray classes. Other options such as increasing brightness is also not applied as X-ray scans are generally similar in both currently used dataset as well as in real-life practice.

The usual train test split is used instead of stratified split as the preservation of class proportion is not desired due to the imbalance of samples as mentioned. Aside from training purposes, the training set is also sampled and passed to the same pre-processing function used in training to provide visualizations of CXR scans after being processed.

B. Data Pre-processing

Equations in display format are separated from the paragraphs of the text. Equations should be flushed to the left of the column. Equations should be made editable. Displayed equations should be numbered consecutively, using Arabic numbers in parentheses. See Eq. (1) for an example. The number should be aligned to the right margin.

Based on randomly sampled observations, all images are perfectly collected for training, with no visible defects that might significantly impact the model's performance. Thus, no images have been dropped from the original dataset. Normalization is performed on both training and test datasets by enabling the rescale parameter (rescale = 1./255) which converts the pixels within the range from [0, 255] to [0, 1]. This scaling procedure aids in making images contribute more evenly to the calculated total loss. The low range also helps in increasing the likeliness of the neural network to converge.

The input (training and test) images are also resized uniformly to 256 by 256 by specifying the input shape parameter in the first layer of the Keras sequential model.

Three pre-processing methods have been chosen as the differentiating variable for each model, which are CLAHE, histogram equalization [20] and no pre-processing. CLAHE and histogram equalization are image enhancement methods used to bring out distinguishing features that might be important for deep learning models to capture thus building their knowledge base on the classes within the dataset. Both pre-processing methods are implemented using the OpenCV API. CLAHE stands for Contrast Limited Adaptive Histogram Equalization and is a subset of adaptive histogram equalization. It is used primarily to improve contrast in images akin to the usual histogram equalization with a slight difference in approach. Instead of using the entire image, CLAHE computes multiple histograms by focusing on small regions within an image called tiles. These tiles correspond to local areas within distinct sections of the image which redistributes the lightness value of the image. This results in improved contrast, further enhancing the boundaries or edges that will be useful in capturing distinguishing shape of lung abnormalities within the CXR scans. CLAHE is an improved version of adaptive histogram equalization, in which it solves the problem of over amplifying noise in homogenous areas. This is done by the introduction of contrast limit that clips calculated histogram. The clipping process is performed before the calculation of Cumulative Distributive Function (CDF) [19]. This clipping variable is set in the pre-processing of input images phase for the first model by specifying the clip limit (CL) to be 4 using the OpenCV API. The number of tiles were kept the same as the default value specified by OpenCV which is (8,8).

Histogram equalization is an umbrella term that can be used to refer to various subsets of image enhancement using similar methodologies. However, in this experiment histogram equalization used as the manipulated variable for the second model refers to the traditional form of histogram equalization. The method contrasts itself with its aforementioned subset, CLAHE where it only uses one histogram that represents the whole image for the purpose of enhancement. These histograms are then equalized, resulting in a distribution of intensity values across the entire image. Regions with lower contrasts will then be able to increase its contrast as a result. Histogram equalization works particularly well with images with dark background and lighter coloured subjects such as XRay scans. It also has the advantage of being computationally cheaper compared to its more complex subset due to its fairly straightforward approach. The CDF of a standard histogram is given as H'(i):

$$H'(i) = \sum_{0 \le j < i}^{X} H(j) \quad (1)$$

This equation is then used to remap the histogram by normalizing H'(i) to have a maximum value of 255. Next, the intensity values for the histogram equalized image can be obtained using the following equation:

$$\text{equalized}(x,y) = H'(\text{src}(x,y)) \quad (2)$$

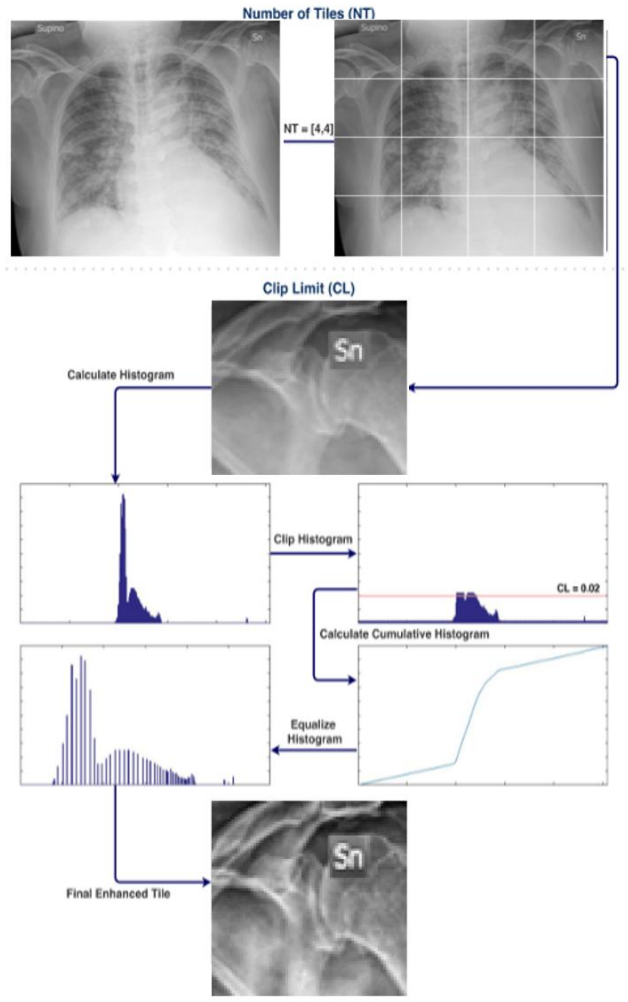

Fig. 1. The process of applying CLAHE.

All models are fed with CXR scans that have been processed into a grayscale image using the OpenCV cvtColor method. Fig. 1 demonstrates the process of applying CLAHE (Contrast Limited Adaptive Histogram Equalization) to a chest X-ray image. Below is a detailed explanation of each step in the diagram:The first step involves dividing the chest X-ray image into a 4x4 grid, resulting in 16 smaller tiles.

This division is done to allow local contrast enhancement, which is the main feature of CLAHE. In the diagram, the original chest X-ray image is shown, and the grid overlay highlights the individual tiles. The next step involves setting a clip limit (CL). The clip limit controls the amount of contrast enhancement applied during CLAHE. A higher clip limit leads to greater contrast enhancement. In this flowchart, the clip limit is set to CL = 0.02. For each tile, a histogram is calculated. A histogram represents the distribution of pixel intensity values in the image. This step is important because CLAHE works by

manipulating the image's histogram to enhance the contrast in areas of the image with low contrast. After calculating the histogram, the clip histogram step follows. In this step, the histogram is clipped to the defined clip limit. If any part of the histogram exceeds the clip limit, it is clipped off and redistributed, effectively limiting the maximum intensity range. This helps in preventing over-enhancement of certain regions and preserving the details in the image.

This cumulative distribution function (CDF) represents the cumulative sum of the clipped histogram. It helps in redistributing the pixel intensities across the entire range, which further contributes to improving the local contrast.The equalization step follows the cumulative histogram calculation. Here, the pixel intensities are redistributed based on the cumulative histogram. This process enhances the contrast in the image by stretching the pixel intensity values over a wider range. The equalized histogram allows for a more balanced distribution of pixel values, making the image more visually appealing and improving the visibility of important features. The final step shows the enhanced tile after applying CLAHE. The local contrast of the selected tile has been enhanced, making the details of the image more visible. In this case, the tile with the "Sn" label (possibly representing a specific area of interest in the X-ray image) is shown as the final enhanced tile.

C. Descriptive Analysis

Samples of processed images have been by extracting images from the training dataset and passing it through the same image processing methods used in the training of the model. We can see the difference in the resulting images after being passed through different image processing methods as following Fig. 2:

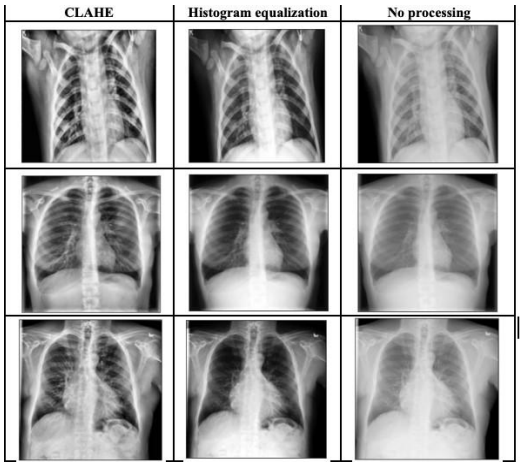

Fig. 2. Images after pre-processed with different image enhancement methods.

Through observation, both CLAHE and histogram equalization has helped in highlighting the edges and the shape of lung opacities when present in CXR scans. Differences in between CLAHE and histogram equalization are as expected, where histogram equalization tends to subdue the intensity of homogenous areas (pixel with similar values). This can be described based on the third row of sample images, where the ribcages at the center of the histogram equalized image is seen to almost lose its shape due to lowered contrast. CLAHE on the other hand seems to uniformly enhance its features, consistently providing clearer shape of the ribcages. We can also see that CLAHE tends to highlight the structures within white areas better compared to histogram equalized images. This may improve its chance in building a better predictor. It may also backfire as no mention of inner structures of lung opacity is mentioned to be a signal or indicator that can be used to distinguish different pneumonia diseases. This means that these enhanced inner structures might become irrelevant features in the process of identification.

D. Modelling to Data

Three different CNN models have been developed to fulfil the purpose of this paper. All models are constructed using the sequential model class from Keras with the same structure which consists of two convolutional layers, two max pooling layers, one flattening layer and two dense layers.

The convolutional layers are purposely built to have increasing number of filters as the inputs are passed deeper into the CNN model. This is done to capture larger numbers of patterns to enable the model in identifying greater nuances within the CXR scans. Convolutional layers are all proceeded by max pooling layers throughout the structure. Max pooling is immediately applied to the first layer of the CNN structure to downsample input images, reducing dimensions and learnable parameters. This helps in decreasing the amount of time needed to train the classification model. The overall structure can be visualized using the VisualKeras library as follows in Fig. 3:

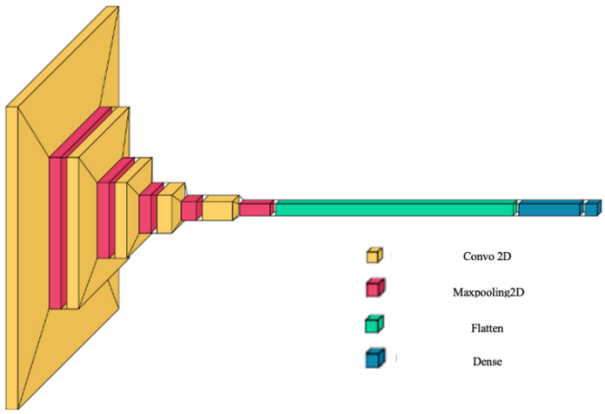

Fig. 3. Resized structure of the CNN models used in the experiment.

Normalization: Normalization is a process in data preprocessing which is used to change the range of numerical data so that it is located in a specific cell, such as [0,1] or [1,1]. In image processing, normalization is a common practice. The essence of the method is some layer input data of the neural network that is preprocessed with zero mathematical expectations and unit variance with the intention of improving the stability and efficiency of the training process [10]. For FER tasks, normalization can give different features similar to ranges. Unnormalized data may lead to unstable gradient problems during model training. In deep learning models, normalized data may lead to a gradient that is too large or too small, thus affecting the learning effect of the model. The normalization in FER2013 dataset is shown in Fig. 8:

Over categorical in this experiment due to the mutually exclusive nature of the dataset classes. This means that the true classes (Yi) are encoded as standalone integers instead of onehot encoded. Examples of true classes for sparse categorisation are [1], [2], [3] while one-hot encoded true classes are [1,0,0], [0,1,0], [0,0,1]. The true classes in sparse categorisation refer to the indices of the classes. Linking the class prediction of a model is done by taking the ground truth. For example, if a model output is [0.5, 0.2, 0.4], the prediction will be class 1 if the class indexation starts from 1. The cross-entropy equation is the same, with the only difference being the format of the true class labels:

$$J(w) = -\frac{1}{N}\sum_{i=1}^{N} y_i \log(\hat{y}_i) \quad (3)$$

Where:y_i = true label, $\hat{y}_i$ = predicted label, W = model parameters.

To avoid overfitting, several options have been considered for data regularization such as adding a dropout layer, adding a normalization layer after the input layer, as well as adding a kernel regularizer in the last layer. Ultimately, it has been decided the only regularizer that will be used is the Ridge Regression regularizer (L2 regularization). The decision to not use normalization layer is due to significant drop in performance for all models when applied. Dropout layer has also been experimented but also disregarded due to similar drop in performance. Dropout layer has also been found to be more effective when used with deeper deep learning structures. The L2 regularization was chosen over L1 regularization as it does not have the tendency to completely remove features deemed as irrelevant. This behaviour is because L1 is capable of forcing coefficients to be exactly zero if given high enough tuning parameter value (usually denoted by λ). While this might be good in reducing the possibility of overfitting in most cases, L1 is not used in this experiment to preserve every single parameter no matter how insignificant and only measure their respective importance by their coefficient values. This decision is made to avoid removing possibly important nuances that might help in the final classification process.

Three options of optimizers have been considered, namely Adaptive Moment Optimization (Adam), stochastic gradient descent (SGD) and Root Mean Squared Propagation (RMSProp). After performing multiple iterations using a controlled model with the same structure, Adam has been chosen due to its excellent performance. It has also been chosen based on its efficiency when working with large datasets. Adam inherits the same concept of momentum from gradient descent with momentum, usually denoted by mt. The formula is given as follows:

$$m_t = \beta_1 m_{t-1} + (1-\beta_1)\left[\frac{\delta L}{\delta w_t}\right] \quad (4)$$

Where:m_t = aggregate of gradients at time t [current], m_{t-1} = aggregate of gradients at time t-1 [previous],w_t= weights at time t, δL = derivative of Loss Function, δw_t = derivative of weights at time t, β_1= moving average parameter.

It also inherits the use of exponential moving average from RMSProp, giving us a new variable called sum of square of past gradients, denoted by vt.

$$v_t = \beta_2 v_{t-1} + (1-2)\left[\frac{\delta L}{\delta w_t}\right]^2 \quad (5)$$

Where:v_t = sum of square of past gradients,β_2 = moving average parameter.

Adam further improves on these variables by computing and using bias corrected versions of the variables. These new variables are given as follows:

$$\widehat{m_t} = \frac{m_t}{1-\beta_1^t} \quad (6)$$

$$\widehat{v_t} = \frac{v_t}{1-\beta_2^t} \quad (7)$$

The weights are then updated using the following equation:

$$w_t = w_t - \widehat{m_t}\left(\frac{\alpha}{\sqrt{\widehat{v_t}+\varepsilon}}\right) \quad (8)$$

Where: ϵ = a small + ve constant to avoid 'division by 0' error.

When training a deep learning model, the training accuracy rate and validation accuracy rate are important indicators to measure the model performance. The training accuracy rate refers to the proportion of correct predictions of the model on the training data set during the training process. It reflects the model's performance on known training data. The validation accuracy rate refers to the prediction accuracy rate of the model on the validation set. Validation sets are data that have not been seen before in the training process and are mainly used to evaluate the generalization ability of the model.

$$\text{Train Acc} = \frac{\sum_{i=1}^{n} 1(\hat{y}_i = y_i)}{n} \times 100 \quad (9)$$

$$Val\ Acc = \frac{\sum_{i=1}^{m} 1(\hat{y}_i = y_i)}{m} \quad (10)$$

Where, for each training sample x_i the model's prediction $\hat{y}_i$, $y_i$is compared with the true label. If the prediction is correct, that counts as a correct prediction.

Due to the sheer variations of model that can be generated by varying the value of hyperparameters in CNN, cross-validation and hyperparameter tuning using GridSearchCV or RandomSearchCV has not been applied. This decision was made considering the computational costs involved as well as time constraints. However, hyperparameter tuning has been done manually to increase the performance of each model. The final values of hyperparameters are listed as below in Table I:

TABLE I. FINAL HYPERPARAMETERS CHOSEN FOR CNN MODELS

Hyperparameter	Value
Batch size	32
Epoch	25
Adam learning rate	0.001
Adam β_1	0.9
Adam β_2	0.999
Adam ε	0.0000007
L2 regularizer λ	0.01
CLAHE clip limit	4

E. Communicating and Visualizing the Results

As shown in Fig. 4, both Train Loss and Val Loss decrease gradually with the training rounds. The validation loss fluctuates at some points, but the overall trend is also downward. The CLAHE-enhanced model showed a good decreasing trend of training and verification loss, indicating that the model gradually learned the features on the training set and verification set. The training accuracy (Train Acc) and validation accuracy (Val Acc) both increased steadily, and basically became stable when they approached 20 epochs, indicating that the verification accuracy and training accuracy were close to each other, indicating that the model avoided overfitting well, and CLAHE enhancement helped the model learn image features better [5].

As shown in Fig. 5, training losses and validation losses decreased gradually, and validation losses also fluctuated in some epochs, but the overall trend was downward. Compared with the CLAHE-enhanced model, the validation loss fluctuation is slightly larger, indicating that the model has a slightly weak generalization ability on the validation set and may need further tuning. Training accuracy and validation accuracy rise rapidly in the initial phase and level off near 20 epochs. The verification accuracy is slightly lower than the training accuracy, which indicates that the performance of the model on the verification set is slightly worse than that on the training set, and there is a certain tendency of overfitting, but the overall performance is still good.

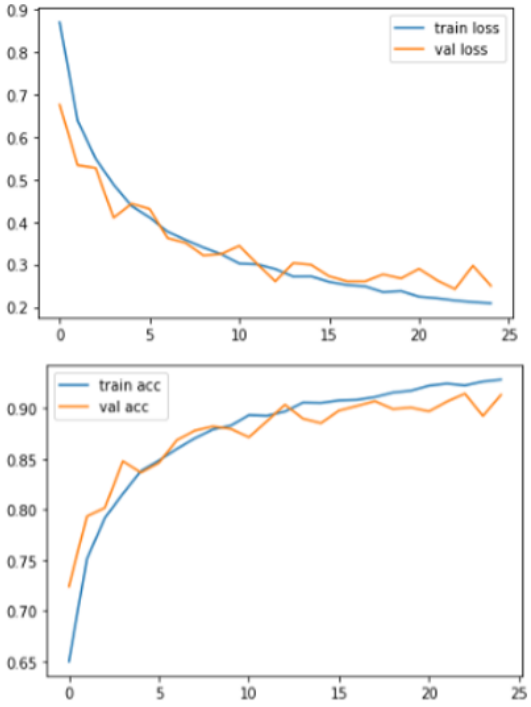

Fig. 4. Images after pre-processed with different image enhancement methods (I).

As shown in Fig. 6, Training losses and validation losses also decrease with epoch, and validation losses also fluctuate at some points, but less so. The loss of the model without preprocessing decreased relatively gradually, especially after 10 epochs, and the validation loss was sometimes slightly higher than the training loss, indicating that the model needed longer training time to reach a stable state without preprocessing. Despite the high accuracy on the validation set, it performed slightly worse than models preprocessed with CLAHE and histogram equalization, suggesting that data without preprocessing may result in a limited ability of the model to learn features as well as it would have done with preprocessing techniques.

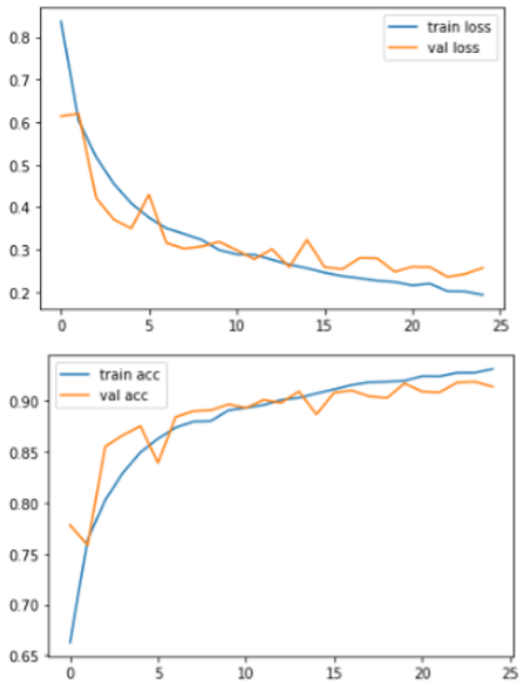

Fig. 5. Images after pre-processed with different image enhancement methods (II).

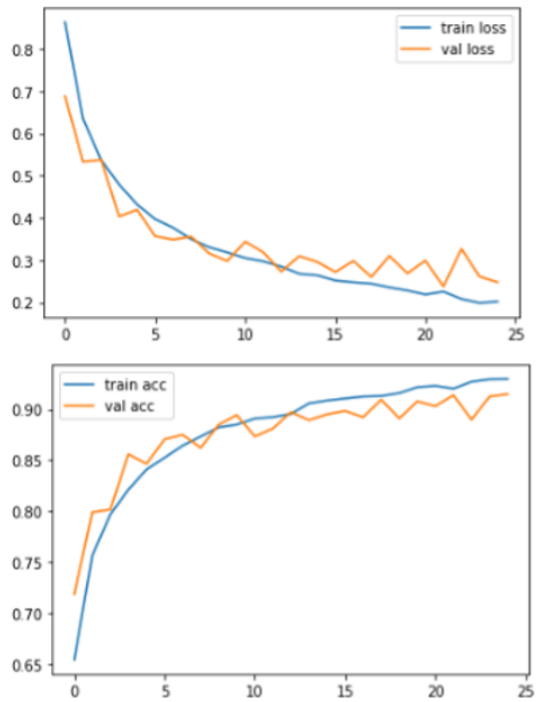

Fig. 6. Images after pre-processed with different image enhancement methods (III).

Image preprocessing has a significant effect on the performance of the model. CLAHE enhancement technology works best at improving local contrast, helping models better learn useful features to improve accuracy and reduce overfitting.

Histogram equalization came in second, while models without any preprocessing performed poorly. It is suggested to use appropriate image preprocessing technology in practical application to improve the generalization ability and overall performance of the model.

IV. RESULTS

The Table II outlines the performance of each model based on the predefined evaluation metrics above.

TABLE II. PERFORMANCE OF EACH MODEL

Image enhancement	Accuracy (%)	Validation accuracy (%)	Loss	Validation loss
CLAHE	93.26	91.31	0.1987	0.2503
Histogram equalization	93.16	91.42	0.1935	0.2569
No preprocessing	92.98	91.50	0.2020	0.2479

Based on the final results obtained, we can observe that all four evaluation metric scores for all of the models are relatively the same.

As shown in Table III. CLAHE performs the best at training, with the highest accuracy score and second lowest loss. The difference between models using histogram equalized inputs and no pre-processing is relatively minor, where no preprocessing scores 0.18 lower accuracy and 0.0085 higher loss. CLAHE scored 0.28 and 0.1 higher in training accuracy compared to no pre-processing and histogram equalized models respectively. CLAHE also has the second-best loss with a 0.0052 and 0.0032 margin compared to no histogram equalized and no pre-processing models. However, evaluation metrics based on the validation data set tells a different story, with CLAHE being the worst performer, with validation accuracy of 91.31 and a 0.0024 higher loss compared to no pre-processing. Interestingly, the model trained using inputs without any form of image processing became the best performer with a validation accuracy score of 91.50 and validation loss of 0.2479. This contradicts with initial hypothesis based on literature reviews, that CLAHE would be the best performer in both training and validation phase. Upon consideration, histogram equalization is chosen as the best method to enhance CXR scans for this very specific CNN model. The main reason to this choice is due its overall performance during both training and validation phase. Models that are better at validation usually signifies a better capability to generalise. Specifically for the context of this experiment, histogram equalization enables the model to better identify distinguishing features that characterise COVID-19 inflicted CXR scans instead of 'memorizing' the features through training datasets without actual 'understanding'. The fact that CLAHE is better at enhancing the minute details of lung abnormalities might the drawback to its ability to generalize as well as histogram equalized model and no preprocessing model.

TABLE III. EVALUTION METRIC MEAN AND STANDARD DEVIATION CLAHE

Metric	Mean	Standard deviation
Training accuracy	0.869348	0.079467384
Training loss	0.351748	0.189184685
Validation accuracy	0.872868	0.044526815
Validation loss	0.34308	0.107216724

Table IV shows the histogram equalization model. the mean value of the training accuracy rate is 0.880868, and the standard deviation is 0.061541603, showing a high training accuracy rate, while the standard deviation is small, indicating that the training process is relatively stable. The average verification accuracy is 0.885632, and the standard deviation is 0.040508844. The verification accuracy is high and the fluctuation is small, indicating that the model has good generalization ability. The validation loss is 0.32322 with a standard deviation of 0.102009803, showing large fluctuations on some validation data, but still performing well overall. Histogram equalization improves the performance of the model, especially in the validation accuracy, but the validation loss fluctuates greatly, suggesting that its stability is slightly lower than that of CLAHE.

TABLE IV. EVALUTION METRIC MEAN AND STANDARD DEVIATION HISTOGRAM EQUALIZATION

Metric	Mean	Standard deviation
Training accuracy	0.880868	0.061541603
Training loss	0.323184	0.148779061
Validation accuracy	0.885632	0.040508844
Validation loss	0.32322	0.102009803

Table V shows that the mean training accuracy of the model without preprocessing is 0.876968, and the standard deviation is 0.063891847, indicating that the consistency in the training process is good, but the accuracy of the model is slightly lower than that of other preprocessing methods. The average validation accuracy is 0.875144, and the standard deviation is 0.044533499, which is close to the validation accuracy compared with other methods, but slightly lower than CLAHE and histogram equalization methods. The verification loss is 0.343188 and the standard deviation is 0.104845224. The fluctuation of the verification loss is large, which shows the instability of the model on the verification set.

TABLE V. EVALUTION METRIC MEAN AND STANDARD DEVIATION WITH NO-PREPROCESSING

Metric	Mean	Standard deviation
Training accuracy	0.876968	0.063891847
Training loss	0.335916	0.155654603
Validation accuracy	0.875144	0.044533499
Validation loss	0.343188	0.104845224

V. DISCUSSION

During the training phase, the CLAHE-enhanced model outperformed both the histogram equalization and no preprocessing models in terms of accuracy, achieving a training accuracy of 93.26%. This suggests that CLAHE excels in enhancing the minute details of lung abnormalities, which could be crucial in detecting subtle features associated with COVID-19 infections. The model's relatively low loss (0.1987) further emphasizes its ability to minimize errors during training.

However, the histogram equalization method, while slightly less effective than CLAHE in terms of training accuracy, performed well with a mean training accuracy of 93.16%. This method helped improve the contrast and brightness of CXR images, which may have helped the model more effectively learn the distinguishing features of the images. Notably, the training loss for histogram equalization (0.1935) was also lower than that of the CLAHE-enhanced model, suggesting that while CLAHE improves feature details, histogram equalization might be more effective at optimizing the overall model performance by reducing error rates during training.

The model without preprocessing, while achieving a slightly lower training accuracy (92.98%), showed stable training consistency. With a training loss of 0.2020, it demonstrated that even without preprocessing, the CNN model could still effectively learn to classify the CXR images, albeit with less precision than the other methods. This highlights that while preprocessing enhances model performance, it is not an absolute requirement for effective training.

The validation phase results presented a different picture, where the CLAHE-enhanced model performed the worst in terms of validation accuracy (91.31%) and exhibited the highest validation loss (0.2503). This is in contrast to the initial hypothesis, which anticipated that CLAHE would perform well in both training and validation phases. The discrepancy between training and validation performance suggests that while CLAHE is effective in fine-tuning the model's ability to capture minute details in CXR images, it might lead to overfitting. The enhanced features could cause the model to 'memorize' training data without fully generalizing to unseen validation images, thus impairing its performance on the validation set.

In contrast, the model trained without any preprocessing achieved the best validation accuracy (91.50%) and the lowest validation loss (0.2479), despite its lower training accuracy compared to CLAHE. This indicates that the lack of preprocessing enabled the model to generalize better, as it did not overfit the specific features of the training set. The validation results for this model demonstrate that preprocessing methods like CLAHE and histogram equalization might enhance feature extraction but at the cost of generalization ability. These findings highlight the importance of balancing training performance with generalization, especially in medical image classification, where the model must perform well on unseen data.The histogram equalization model, while showing good validation accuracy (91.42%), also exhibited noticeable fluctuations in validation loss (0.2569). While histogram equalization improved the model's ability to generalize better than CLAHE, it still presented challenges in terms of stability during the validation phase. The slightly better performance of the histogram equalization model, compared to CLAHE, underscores its ability to enhance image contrast while maintaining reasonable generalization.

VI. CONCLUSION

This study evaluated the impact of different image preprocessing techniques—CLAHE, traditional histogram equalization, and no preprocessing—on the performance of a convolutional neural network (CNN) for COVID-19 classification using chest X-ray (CXR) images. The experimental results demonstrated that all preprocessing methods improved model performance during the training phase, but the validation phase revealed distinct trade-offs between accuracy, loss, and generalization ability.

The CLAHE-enhanced model achieved the highest training accuracy (93.26%) and exhibited strong stability, but it showed poor generalization in the validation phase, with the lowest validation accuracy (91.31%) and higher validation loss (0.2503). This suggests that while CLAHE helps capture detailed image features, it may lead to overfitting, affecting the model's ability to generalize effectively. In contrast, the model without preprocessing achieved the best validation performance, with a validation accuracy of 91.50% and the lowest validation loss (0.2479), highlighting its superior generalization ability. However, its training accuracy (92.98%) was slightly lower compared to the other methods. This finding emphasizes that while preprocessing enhances feature extraction, a simpler, unprocessed approach can sometimes yield better generalization.

The histogram equalization method, while not the best in training accuracy, provided a good balance between training performance and validation accuracy. With a validation accuracy of 91.42%, it demonstrated that traditional image enhancement techniques could improve generalization without overfitting, making it the most suitable preprocessing method for the CNN model in this study.

In conclusion, histogram equalization emerged as the optimal preprocessing method for COVID-19 classification in CXR images, offering the best combination of training and validation performance. Future work could investigate more sophisticated preprocessing techniques or hybrid models to further enhance both performance and generalization in medical image classification tasks.

VII. FUTURE WORKS AND LIMITATION

While this study has provided valuable insights into the effect of image preprocessing techniques on COVID-19 detection using chest X-ray (CXR) images, there are several avenues for future research to further enhance the performance and generalization of deep learning models. 1.Future work could explore combining CLAHE and histogram equalization to leverage the strengths of both methods. A hybrid preprocessing approach could potentially enhance image details while maintaining good generalization ability, addressing the limitations seen when using CLAHE alone. 2. The use of more sophisticated deep learning models, such as ResNet, DenseNet, or Inception networks, may further improve performance, especially in terms of handling complex features in CXR images.These architectures have been shown to excel at feature

extraction and overcoming challenges like overfitting. 3.To address the potential overfitting issues observed, further research could incorporate advanced data augmentation techniques. This could include random rotations, flips, and color jittering, or even synthetic data generation techniques, to create a more diverse training dataset and enhance the generalization capability of the model. 4. Future research should focus on testing these models in real-world clinical environments to evaluate their robustness, scalability, and performance on larger, diverse datasets. This would also include the development of a user-friendly interface for healthcare professionals to easily adopt the models in practice.

This study has several limitations that should be addressed in future work. 1. The model was trained using a limited number of CXR images from the COVID-19 Radiography Database. Although the dataset is large, it may not fully represent the variety of CXR images encountered in real-world clinical settings, which could impact the model's ability to generalize to diverse populations and varying image qualities. Expanding the dataset or incorporating additional datasets from other regions or healthcare providers could improve the model's robustness. 2. While different preprocessing techniques were evaluated, the impact of each preprocessing method may vary depending on the dataset used. The methods tested in this study may not perform equally well on other datasets or in clinical settings. Therefore, the generalizability of these findings across different datasets remains an open question. 3. While deep learning models, including CNNs, are powerful for image classification tasks, they are often criticized for their lack of interpretability. Future work should focus on making the models more explainable to healthcare providers. Techniques such as Grad-CAM (Gradient-weighted Class Activation Mapping) can be employed to visualize which parts of the CXR images are contributing to the model's predictions, making the model more transparent and aiding in clinical decision-making. 4. This study focused solely on the detection of COVID-19 from CXR images, and did not account for other variables that may affect the model's performance, such as different scanner types, patient positioning, or image resolution. These external factors can significantly influence model accuracy and should be considered in future studies for a more comprehensive evaluation of the model's real-world effectiveness.

ACKNOWLEDGMENT

Funding: This research was funded by the Universiti Kebangsaan Malaysia (Grant code: GUP-2022-060).

Author Contributions: The authors confirm contribution to the paper as follows: study conception and design: Ahmad Nuruddin bin Azhar and Nor Samsiah sani; data collection: Ahmad Nuruddin bin Azhar; analysis and interpretation of results: Ahmad Nuruddin bin Azhar, Liu Luan Xiang Wei and Nor Samsiah sani; draft manuscript preparation: Mohd Aliff Afira Sani, Liu Luan Xiang Wei and Nor Samsiah sani. All authors reviewed the results and approved the final version of the manuscript.

Conflict of Interest The corresponding author states that there is no conflict of interest on behalf of all authors.

Data Availability: The data used in this study are available from the following resources in the public domain:

https://www.kaggle.com/datasets/tawsifurrahman/covid19radiography-database.

REFERENCES

[1] Dobrojevic, M., Zivkovic, M., Chhabra, A., Sani, N. S., Bacanin, N., & Amin, M. M. (2023). Addressing internet of things security by enhanced sine cosine metaheuristics tuned hybrid machine learning model and results interpretation based on shap approach. PeerJ Computer Science, 9, e1405.

[2] Suwadi, N. A., Derbali, M., Sani, N. S., Lam, M. C., Arshad, H., Khan, I., & Kim, K. I. (2022). An optimized approach for predicting water quality features based on machine learning. Wireless Communications and Mobile Computing, 2022(1), 3397972.

[3] Othman, Z. A., Bakar, A. A., Sani, N. S., & Sallim, J. (2020). Household overspending model amongst B40, M40 and T20 using classification algorithm. International Journal of Advanced Computer Science and Applications, 11(7).

[4] Mohamed Nafuri, A. F., Sani, N. S., Zainudin, N. F. A., Rahman, A. H. A., & Aliff, M. (2022). Clustering analysis for classifying student academic performance in higher education. Applied Sciences, 12(19), 9467.

[5] Holliday, J., Sani, N., & Willett, P. (2018). Ligand-based virtual screening using a genetic algorithm with data fusion. Match: Communications in Mathematical and in Computer Chemistry, 80(3).

[6] Bassel, A., Abdulkareem, A. B., Alyasseri, Z. A. A., Sani, N. S., & Mohammed, H. J. (2022). Automatic malignant and benign skin cancer classification using a hybrid deep learning approach. Diagnostics, 12(10), 2472.

[7] Z. Liu et al., "Near-real-time monitoring of global CO2 emissions reveals the effects of the COVID-19 pandemic," Nat. Commun., vol. 11, no. 1, 2020, doi: 10.1038/s41467-020-18922-7.

[8] V. J. Jayaraj, S. Rampal, C. W. Ng, and D. W. Q. Chong, "The Epidemiology of COVID-19 in Malaysia," Lancet Reg. Heal. - West. Pacific, vol. 17, 2021, doi: 10.1016/j.lanwpc.2021.100295.

[9] S. Dilshad et al., "Automated image classification of chest X-rays of COVID-19 using deep transfer learning," Results Phys., vol. 28, 2021, doi: 10.1016/j.rinp.2021.104529.

[10] A.Waheed, M. Goyal, D. Gupta, A. Khanna, F. Al-Turjman, and P. R. Pinheiro, "CovidGAN: Data Augmentation Using Auxiliary Classifier GAN for Improved Covid-19 Detection," IEEE Access, vol. 8, 2020, doi: 10.1109/ACCESS.2020.2994762.

[11] L. A. Rousan, E. Elobeid, M. Karrar, and Y. Khader, "Chest x-ray findings and temporal lung changes in patients with COVID-19 pneumonia," BMC Pulm. Med., vol. 20, no. 1, 2020, doi: 10.1186/s12890020-01286-5.

[12] C. Oterino Serrano et al., "Pediatric chest x-ray in covid-19 infection," Eur. J. Radiol., vol. 131, 2020, doi: 10.1016/j.ejrad.2020.109236.

[13] A.I.K., A. R., U. Patel, and S. K. Joshi, "H1N1 influenza: Characterization of initial chest radiographic findings and prognostic value of serial chest radiographs," Radiol. Infect. Dis., vol. 3, no. 4, 2016, doi: 10.1016/j.jrid.2016.11.005.

[14] M. E. H. Chowdhury et al., "Can AI Help in Screening Viral and COVID-19 Pneumonia?," IEEE Access, vol. 8, 2020, doi: 10.1109/ACCESS.2020.3010287.

[15] H. Mary Shyni and E. Chitra, "A COMPARATIVE STUDY OF X-RAY AND CT IMAGES IN COVID-19 DETECTION USING IMAGE PROCESSING AND DEEP LEARNING TECHNIQUES,"Comput. Methods Programs Biomed. Updat., vol. 2, 2022, doi:10.1016/j.cmpbup.2022.100054.

[16] T. Rahman et al., "Exploring the effect of image enhancement techniques on COVID-19 detection using chest X-ray images," Comput. Biol. Med., vol. 132, 2021, doi: 10.1016/j.compbiomed.2021.104319.

[17] K. Hasikin and N. A. M. Isa, "Enhancement of the low contrast image using fuzzy set theory," 2012. doi: 10.1109/UKSim.2012.60.

[18] M. Selvi and A. George, "FBFET: Fuzzy based fingerprint enhancement technique based on adaptive thresholding," 2013. doi: 10.1109/ICCCNT.2013.6726776.

[19] W.-N. Mohd-Isa, J. Joseph, N. Hashim, and N. Salih, "Enhancement of digitized X-ray films using Contrast-Limited Adaptive Histogram Equalization (CLAHE)," F1000Research, vol. 10, 2021, doi: 10.12688/f1000research.73236.1.

[20] G. F. C. Campos, S. M. Mastelini, G. J. Aguiar, R. G. Mantovani, L. F. de Melo, and S. Barbon, "Machine learning hyperparameter selection for Contrast Limited Adaptive Histogram Equalization," Eurasip J. Image Video Process., vol. 2019, no. 1, Dec. 2019, doi: 10.1186/s13640019-0445-4.

[21] A. Agnihotri and N. Kohli, "A Hybrid Deep Neural approach for multi-class Classification of novel Corona Virus (COVID-19) using X-ray images," in *2023 International Conference on Advancement in Computation & Computer Technologies (InCACCT)*, Gharuan, India: IEEE, May 2023, pp. 1–5. doi: 10.1109/InCACCT57535.2023.10141782.

[22] F. Bougourzi, F. Dornaika, A. Nakib, C. Distante, and A. Taleb-Ahmed, "Deep-Covid-SEV: an Ensemble 2D and 3D CNN-Based Approach for Covid-19 Severity Prediction from 3D CT-SCANS," in *2023 IEEE International Conference on Acoustics, Speech, and Signal Processing Workshops (ICASSPW)*, Rhodes Island, Greece: IEEE, Jun. 2023, pp. 1–5. doi: 10.1109/ICASSPW59220.2023.10192927.

[23] E. Dandil and M. S. Yildirim, "Automatic Segmentation of COVID-19 Infection on Lung CT Scans using Mask R-CNN," in *2022 International Congress on Human-Computer Interaction, Optimization and Robotic Applications (HORA)*, Ankara, Turkey: IEEE, Jun. 2022, pp. 1–5. doi: 10.1109/HORA55278.2022.9800029.

[24] H. Hammad and H. Khotanlou, "Detection and visualization of COVID-19 in chest X-ray images using CNN and Grad-CAM (GCCN)," in *2022 9th Iranian Joint Congress on Fuzzy and Intelligent Systems (CFIS)*, Bam, Iran, Islamic Republic of: IEEE, Mar. 2022, pp. 1–5. doi: 10.1109/CFIS54774.2022.9756420.

[25] B. Khadija, "Automatic detection of covid-19 using CNN model combined with Firefly algorithm," in *2022 8th International Conference on Optimization and Applications (ICOA)*, Genoa, Italy: IEEE, Oct. 2022, pp. 1–4. doi: 10.1109/ICOA55659.2022.9934144.

[26] A. R. A. M and S. R, "Enhancing COVID-19 Diagnosis with Automated Reporting using Preprocessed Chest X-Ray Image Analysis based on CNN," in *2023 2nd International Conference on Applied Artificial Intelligence and Computing (ICAAIC)*, Salem, India: IEEE, May 2023, pp. 35–40. doi: 10.1109/ICAAIC56838.2023.10141515.

[27] P. Maddula, P. Srikanth, P. K. Sree, P. B. V. R. Rao, and P. T. S. Murty, "COVID-19 prediction with Chest X-Ray images using CNN," in *2023 International Conference on Intelligent and Innovative Technologies in Computing, Electrical and Electronics (IITCEE)*, Bengaluru, India: IEEE, Jan. 2023, pp. 568–572. doi: 10.1109/IITCEE57236.2023.10090951.

[28] J. Marusani, B. G. Sudha, and N. Darapaneni, "Small-Scale CNN-N model for Covid-19 Anomaly Detection and Localization From Chest X-Rays," in *2022 First International Conference on Artificial Intelligence Trends and Pattern Recognition (ICAITPR)*, Hyderabad, India: IEEE, Mar. 2022, pp. 1–6. doi: 10.1109/ICAITPR51569.2022.9844184.

[29] R. D. S M, B. S. Rose, S. Akshitha, and P. Niharika, "Comparison of COVID-19 Diagnosis by CNN Model and ResNet Using Chest X-Ray," in *2023 International Conference on Sustainable Communication Networks and Application (ICSCNA)*, Theni, India: IEEE, Nov. 2023, pp. 1569–1574. doi: 10.1109/ICSCNA58489.2023.10370248.

[30] H. Tahir, A. Iftikhar, and M. Mumraiz, "Forecasting COVID-19 via Registration Slips of Patients using ResNet-101 and Performance Analysis and Comparison of Prediction for COVID-19 using Faster R-CNN, Mask R-CNN, and ResNet-50," in *2021 International Conference on Advances in Electrical, Computing, Communication and Sustainable Technologies (ICAECT)*, Bhilai, India: IEEE, Feb. 2021, pp. 1–6. doi: 10.1109/ICAECT49130.2021.9392487.

[31] J. Zhang *et al.*, "Graph Convolution and Self-attention Enhanced CNN with Domain Adaptation for Multi-site COVID-19 Diagnosis," in *2023 45th Annual International Conference of the IEEE Engineering in Medicine & Biology Society (EMBC)*, Sydney, Australia: IEEE, Jul. 2023, pp. 1–4. doi: 10.1109/EMBC40787.2023.10340851.